Aerosol and Air Quality Research

ORIGINAL RESEARCH
https://doi.org/10.4209/aaqr.220145

Changes in Tropospheric Nitrogen Dioxide Vertical Column Densities over Japan and Korea during the COVID-19 Using Pandora and MAX-DOAS

Yongjoo Choi[1*‡], Yugo Kanaya[1], Hisahiro Takashima[1,2], Kihong Park[3], Haebum Lee[3], Jihyo Chong[3,4], Jae Hwan Kim[5], Jin-Soo Park[6]

[1] Research Institute for Global Change, Japan Agency for Marine-Earth Science and Technology, Yokohama 2360001, Japan
[2] Faculty of Science, Fukuoka University, Fukuoka 814-0180, Japan
[3] School of Earth Sciences and Environmental Engineering, Gwangju Institute of Science and Technology, Gwangju 61005, Korea
[4] Environmental Management Division, Yeongsan River Basin Environmental Office, Gwangju 61945, Korea
[5] Department of Atmospheric Sciences, Pusan National University, Busan 46241, Korea
[6] Climate & Air Quality Research Department, National Institute of Environmental Research, Incheon 22689, Korea

ABSTRACT

We investigated the impact of human activity during COVID-19 on the tropospheric nitrogen dioxide vertical column density (NO_2 TropVCD) at three urban sites (Gwangju and Busan in Korea and Yokosuka in Japan) and one remote site (Cape Hedo in Japan) from Multi-Axis Differential Optical Absorption Spectroscopy (MAX-DOAS) and Pandora. Compared to the monthly mean NO_2 TropVCD from 2015 to 2018 and in 2019, the values were lower in 2020 due to social distancing in Korea and Japan. High negative relative changes were observed from May to September (−30% to −18%) at the three urban sites; Cape Hedo, a remote site, did not show a significant difference in relative changes between previous years and 2020, suggesting that only anthropogenic emission sources decreased dramatically. In the case of Yokosuka, the 15-day moving average of the NO_2 TropVCD exhibited a good relationship with transportation (R = 0.48) and industry (R = 0.54) mobility data. In contrast, the NO_2 TropVCD at the Korean sites showed a moderate to low correlation with the industrial sector and insignificant correlations with transportation. The differences in correlations might be caused by the different social distancing policies in Korea (voluntary) and Japan (mandatory). By applying generalized boosted models to exclude meteorological and seasonal effects associated with NO_2 TropVCD variations, we revealed that the decreasing trend from 2019 to 2020 was much steeper than that from 2015 to 2020 (a factor of two), and a significant change was identified in January 2020, when the first cases of COVID-19 were observed in both Korea and Japan. This result confirmed that the reduction in NO_2 can be largely explained by the NO_x emission reduction resulting from social distancing for COVID-19 rather than annual meteorological differences; however, in December 2020, NO_2 recovered suddenly to its previous level due to an increase in human activities.

Keywords: COVID-19, Nitrogen dioxide, MAX-DOAS, Pandora

1 INTRODUCTION

Nitrogen oxides (NO_x = NO_2 + NO) are major components of air quality degradation in urban/industrialized areas due to their role as catalysts in tropospheric ozone formation and as precursors of secondary inorganic aerosols, with consequences for climate and human health

OPEN ACCESS

Received: April 10, 2022
Revised: October 25, 2022
Accepted: March 6, 2023

* **Corresponding Author:**
choingjoo@hufs.ac.kr

‡ **Present address:**
Department of Environmental Science, Hankuk University of Foreign Studies, Gyeonggi 17035, Korea

Publisher:
Taiwan Association for Aerosol Research
ISSN: 1680-8584 print
ISSN: 2071-1409 online

(Crutzen, 1970; Bond *et al.*, 2001; Myhre *et al.*, 2013; Lelieveld *et al.*, 2015). Typically, NO_x is emitted from vegetation fires, lightning, and soils, but emissions from fuel combustion account for ~50% of global total NO_x emissions (Delmas *et al.*, 1997). Because the emission of NO_2 is highly linked with human activities, the NO_2 concentration is comparably higher in urban areas than in rural areas; additionally, NO_x is characterized by a diurnal and weekly cycle in most countries (Beirle *et al.*, 2003; Kanaya *et al.*, 2014), with high NO_2 emissions in rush-hour periods on working days and low NO_2 emissions on weekends or public holidays. As a result of the efforts to limit the effects of deteriorated air quality on public health, emission regulation policies for NO_x and other pollutants have contributed to the reduction of the NO_2 tropospheric vertical column density (TropVCD), which has been confirmed by long-term satellite and ground-based observations (Duncan *et al.*, 2016; Geddes *et al.*, 2016; Georgoulias *et al.*, 2019; Choi *et al.*, 2021).

After coronavirus disease 2019 (COVID-19) first broke out in December 2019 in Wuhan, China, it became an ongoing global pandemic and was deemed a public health emergency of international concern by the World Health Organization (WHO); more than 0.17 billion cases were observed in 212 countries or regions as of 6 June 2021 (WHO, 2020). The dramatical increase in newly confirmed COVID-19 cases globally led to shrinkage in human activities in many countries, which was associated with travel restrictions, self-quarantine measures, curfews, and the closure of businesses and factories to suppress the spread of the virus (Baldasano, 2020; Bauwens *et al.*, 2020; Berman and Ebisu, 2020). From model simulations and satellite observations, the strict regulation period for COVID-19 led to large reductions in the NO_2 TropVCD compared to the level in the same period in 2019; this difference was especially notable for the transportation and industrial sectors (Bauwens *et al.*, 2020; Ding *et al.*, 2020; Forster *et al.*, 2020; Koo *et al.*, 2020; Liu *et al.*, 2020; Miyazaki *et al.*, 2020; Shi and Brasseur, 2020; Venter *et al.*, 2020; Doumbia *et al.*, 2021).

The reduction in the NO_2 TropVCD during the unprecedented COVID-19 period was complicated by several factors, not only changes in anthropogenic emissions rates (e.g., transportation and industrial sectors) but also chemical and meteorological seasonal cycles, generally leading to a decline in NO_2 from winter to spring in the Northern Hemisphere (Martin *et al.*, 2003; Ding *et al.*, 2020; Kroll *et al.*, 2020). Therefore, the reduction in the NO_2 TropVCD driven by COVID-19 must be distinguished from the pre-existing trajectory, and meteorologically driven variability must be considered (Li *et al.*, 2019; Vu *et al.*, 2019; Kroll *et al.*, 2020). Although the satellite-based NO_2 TropVCD can provide valuable estimates over a broad spatial area, there are inherent limitations (e.g., temporal resolution and/or spatially inhomogeneous distribution) that can complement pollutant trends using ground-based measurements (Bechle *et al.*, 2013; Berman and Ebisu, 2020; Choi *et al.*, 2021). Ground-based remote sensing measurements for trace gases (e.g., Multi-Axis Differential Optical Absorption Spectroscopy (MAX-DOAS) and Pandora) have been regarded as ''ground truth'' data for target pollutants and provide higher sensitivity in the lower troposphere and a higher temporal resolution than satellite observations.

In this study, we investigated the impacts of human activity reductions resulting from the spread of COVID-19 on the NO_2 TropVCD at three urban sites (Yokosuka, Japan and Gwangju and Busan, Korea) and one background site (Cape Hedo, Japan); these sites are directly influenced by Chinese and/or local emission sources. In that context, using MAX-DOAS and Pandora instruments, we compared the difference in the NO_2 TropVCD between 2020 (whole year) and that in the previous five years in terms of human activities and meteorological variables. Additionally, we focused on the trend in the NO_2 TropVCD at two different time scales (2015 to 2020 and 2019 to 2020) by decomposing seasonal and weather effects so as to precisely evaluate the NO_x emission reduction.

2 METHODS

2.1 Measurement Sites

We carefully selected the four measurement sites by considering the available multiyear measurements obtained since 2015 over East Asia among the representative ground-based remote sensing measurement networks for trace gases: MAX-DOAS over Russia and Asia (MADRAS; https://ebcrpa.jamstec.go.jp/maxdoashp/) and the Pandonia Global Network (PGN). Fig. 1 shows the geographical locations of the four measurement sites and the differences in the

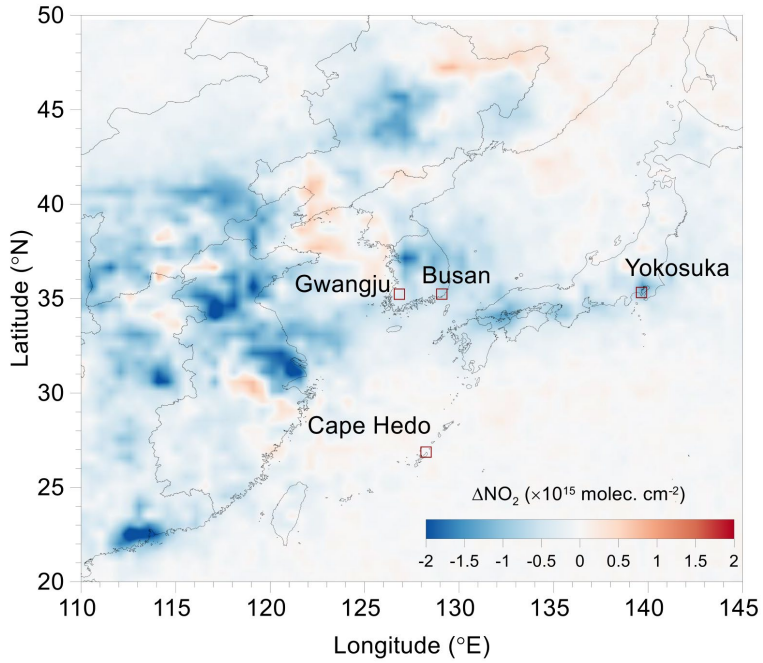

Fig. 1. The difference in tropospheric NO_2 vertical column density (NO_2 TropVCD) over East Asia between 2019 and 2020, which measured by Ozone Monitoring Instrument (OMI) products (OMNO2d_003; solar zenith angle < 80° and cloud fraction < 30%) and site locations of four measurement sites (Yokosuka and Cape Hedo in Japan and Gwangju and Busan in Korea).

NO_2 TropVCD from ozone monitoring instrument (OMI) satellite data (OMNO2d_003) between 2019 and 2020 over East Asia, indicating that the NO_2 TropVCD was reduced in most regions.

The Yokosuka site (139.65°E, 35.32°N) is close to Tokyo and Yokohama, which are two of the largest cities on the Kanto Plain, Japan. According to the Regional Emission inventory in ASia (REAS) version 3.2 (Kurokawa and Ohara, 2020), the NO_x emission rates were 37 Tg in Yokohama (~76% from industry and power plants) and 41 Tg in Tokyo (~49% from road transportation) in 2015. Therefore, the Yokosuka site is suitable for investigating the NO_2 behaviour in urban areas with complex transportation and industrial effects (Kanaya *et al.*, 2014; Choi *et al.*, 2021).

Cape Hedo (128.25°E, 26.87°N) is located in the northernmost part of subtropical Okinawa Island. Because there are no major anthropogenic emission sources at the site (0.02 Tg; ~98% from road transportation in REAS), and this area is distant from local cities (40 km from Nago (population of 60,000) and 100 km from Naha (population of 0.32 million)). Cape Hedo represents a background site in East Asia (Takashima *et al.*, 2009; Kanaya *et al.*, 2014; Choi *et al.*, 2021).

Busan (129.08°E, 35.24°N) is the second-largest city in Korea, with a population of 3.4 million within 770 km^2. The Busan site is located at Pusan National University (PNU), southeastern Korea, and is in a valley surrounded by small mountains. Similar to those in Yokohama, the major NO_x emission sources in Busan are industry and power plants, which account for 65% of the total NO_x emissions.

The Gwangju site (126.84°E, 35.23°N) is located on the campus of the Gwangju Institute of Science and Technology (GIST) in southwestern Korea. Gwangju has a population of 1.5 million people within ~500 km^2 and is one of the metropolitan cities in Korea. The major NO_x emission source near the site is transportation, with a similar contribution (~49%) as that in Tokyo, although the total emission rates in Gwangju in REAS v3.2 are lower than those in Tokyo by a factor of two.

2.2 MAX-DOAS

Information on the MAX-DOAS instrument and its retrieval algorithm has been described in detail elsewhere (e.g., Irie *et al.*, 2008, 2011; Kanaya *et al.*, 2014). MAX-DOAS consists of a light-receiving part and a miniature spectrometer (USB4000; Ocean Optics, Dunedin, FL, USA) connected by a fibre-optic cable bundle. The sky irradiance collected by a telescope is redirected by a prism

reflector and quartz fibre to the spectrometer at six elevation angles (EAs; 3, 5, 10, 20, 30, and 90° (70° for Cape Hedo)) for spectral analysis, with a < 1° field of view (FOV). The prism reflector is sequentially rotated every 5 min for each angle; thus, the measurement interval is 30 min. Among the measured wavelength range (230 to 560 nm, with less than 0.7 nm of full width at half maximum), we chose 460–490 nm for retrieving the NO_2 and oxygen collision complexes (O_2-O_2 or O_4) column densities in this study. For Yokosuka and Cape Hedo, the five-fold optical axes were installed for simultaneous observations at different EAs, but only a single telescope was used for sequential scanning for each EA.

All measured spectra were retrieved by (1) DOAS spectral fittings using QDOAS software version 3.0 and (2) conversion of the differential slant column density (ΔSCD) to TropVCD by optimal estimation methods (Rodgers, 2000). All measurement spectra were first corrected for offset and dark currents and analysed using the DOAS technique to retrieve the ΔSCD of O_4 and NO_2 with respect to the reference spectrum (measured at an EA of 90° or 70° within 30 min). Here, ΔSCD is defined as the difference in the SCD between the measured spectrum and the corresponding reference spectrum. The absorption cross-sections for retrieving the ΔSCD were adopted from Hermans *et al.* (2003) for O_4 but increased by a constant factor of 1.25 (Wagner *et al.*, 2019), Vandaele *et al.* (1996) for NO_2 at 298 K, Bogumil *et al.* (2003) for O_3 at 223 K, Rothman *et al.* (2003) for H_2O, and Chance and Spurr (1997) for Ring effect. A polynomial of degree three was used to fit the continuum.

The ΔSCDs of NO_2 and O_4 were retrieved using MAX-DOAS profile inversion algorithms with the following procedures. The profiles of aerosol optical depth (AOD) at 476 nm below 5 km were retrieved and then used as constraints to retrieve the NO_2 profile below 5 km. To retrieve both the AOD and NO_2 TropVCD, an optimal estimation method (Rodgers, 2000) was applied to solve the nonlinear inversion problem with an iteration equation using a lookup table of box air mass factors (AMFs) that was generated by the Monte Carlo Atmospheric Radiative Transfer Simulator (MCARaTS; Iwabuchi, 2006). In brief, the state vector consisted of the target outputs (AOD or NO_2 TropVCD) and three parameters ($f_{0–1\ km}$, $f_{1–2\ km}$, and $f_{2–3\ km}$; f represents the fractional contribution to the remaining AOD or NO_2 TropVCD from the low-altitude range) used to determine the vertical profiles. Then, each partial column (0–1, 1–2, and 2–3 km) of the target outputs was expressed as $f_{0–1\ km} \times$ output, $(1 - f_{0–1\ km}) \times f_{1–2\ km} \times$ output, and $(1 - f_{0–1\ km}) \times (1 - f_{1–2\ km}) \times f_{2–3\ km} \times$ output. The a priori values of $f_{0–1\ km}$, $f_{1–2\ km}$, and $f_{2–3\ km}$ were 0.60 ± 0.05, 0.80 ± 0.03, and 0.80 ± 0.03, respectively. The a priori values of the AOD and NO_2 TropVCD were 0.21 ± 3.0 and 20% of the largest ΔSCD values for NO_2 among the five ΔSCDs during 30 mins, respectively.

The overall uncertainty in the AOD has been estimated at 30% (Irie *et al.*, 2008; Takashima *et al.*, 2009; Irie *et al.*, 2011) and that in the NO_2 TropVCD has been reported as 17% (Kanaya *et al.*, 2014). The minimum detection limit for the NO_2 TropVCD at an altitude of 0–1 km has been reported to be < 0.2 ppbv, corresponding to 5×10^{14} molecules cm^{-2} (Takashima *et al.*, 2011, 2012; Kanaya *et al.*, 2014). Quality control was carefully conducted to eliminate data measured under abnormal conditions (e.g., changes in integration time and temperature settings, large residuals in the spectral fittings and saturated signal levels) (Kanaya *et al.*, 2014).

2.3 Pandora

Pandora spectrometer was installed at Pusan National University in March 2012 to measure the total column NO_2 and O_3 as part of the Distributed Regional Aerosol Gridded Observation Networks (DRAGON)-Asia campaign in South Korea (Chong *et al.*, 2018). The direct solar beam is measured by Pandora via an optical head sensor attached to a solar tracker and connected to a UV–VIS spectrometer (spectral range of 280–525 nm) by a fibre optic cable attached to the head sensor (Herman *et al.*, 2009, 2019). The direct-sun NO_2 total VCD from Pandora was retrieved by applying a spectral fitting algorithm (Cede, 2019) using a near-noon reference spectrum from which the NO_2 slant column amount is derived by a statistical calibration approach (Herman *et al.*, 2009). The direct-sun NO_2 total VCD has been reported to have high precision and accuracy, and data are available in near-real time as a standard product (Judd *et al.*, 2019); the reported uncertainties of Pandora NO_2 total VCD are ~2.7×10^{14} molecules cm^{-2} for random uncertainty and ~2.7×10^{15} molecules cm^{-2} for systematic uncertainty (Herman *et al.*, 2009). During the CINDI-2 campaign which participated 36 spectrometers, the NO_2 ΔSCD from Pandora instruments at

visible range showed good agreement with reference with small mean relative difference (−1.3% to 3.4%) (Kreher *et al.*, 2020).

Because the NO_2 total VCD contains both stratospheric and tropospheric NO_2 VCDs and most of the NO_2 is located between 0 and 3 km of altitude with only approximately 2.7×10^{15} molecules cm^{-2} (0.1 ± 0.05 DU) in the upper troposphere and stratosphere (Dirksen *et al.*, 2011; Herman *et al.*, 2019), the NO_2 TropVCD from Pandora was derived from the NO_2 total VCD after subtraction of the stratospheric NO_2 VCD estimated using OMI satellite data (Chong *et al.*, 2018; Pinardi *et al.*, 2020). In this study, the Pandora retrievals were screened to exclude observations with uncertainties in NO_2 total VCD greater than 1.35×10^{15} molecules cm^{-2} (0.05 DU) and normalized root-mean square of the weighted spectral fitting residuals greater than 0.005 (Judd *et al.*, 2019; Choi *et al.*, 2020; Pinardi *et al.*, 2020). It should be noted that this approach leads to the retrieval of the total tropospheric column from Pandora, while the tropospheric column from MAX-DOAS mainly represents the boundary layer below 5 km.

3 RESULTS AND DISCUSSION

3.1 Difference in Monthly Variation in the NO_2 TropVCD between 2020 and Previous Years

Fig. 2 shows the monthly mean and standard deviation of the NO_2 TropVCD at four measurement sites during three different time scales: 2015–2018, 2019, and 2020. The monthly mean NO_2 TropVCD in 2020 was generally lower than that in 2015–2018 and in 2019 (some months were not), possibly due to social distancing in South Korea (February) and Japan (April) and the lockdown in China (early in January) to prevent the spread of COVID-19. The relative change in NO_2 in 2020 compared to that in the other periods (2015–2018 and 2019) was calculated using the following equation: $(NO_{2\ \text{in 2020}} - NO_{2\ \text{in other periods}})/NO_{2\ \text{in other periods}}$. For the three urban sites, the relative

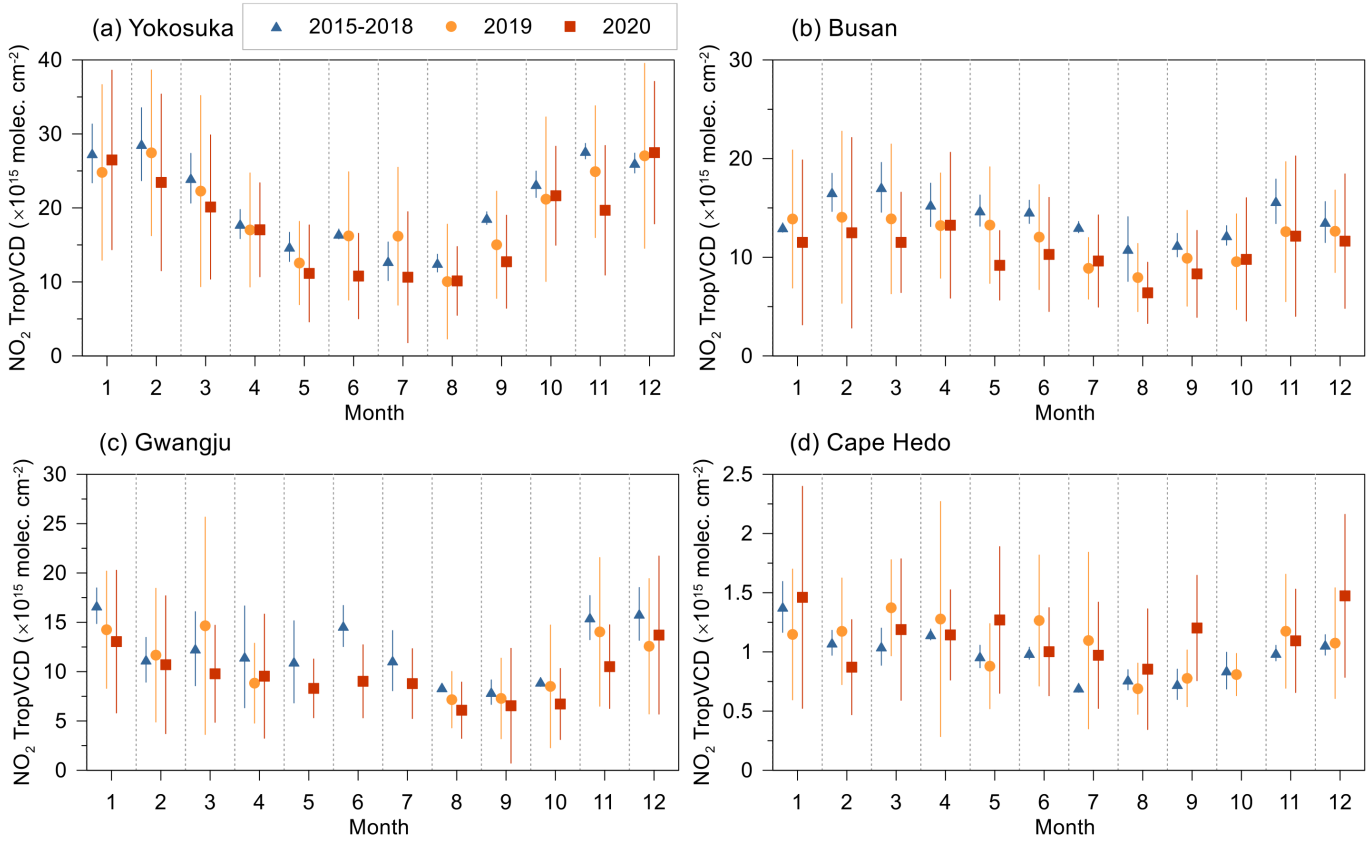

Fig. 2. Monthly variation of NO_2 TropVCD at (a) Yokosuka, (b) Busan, (c) Gwangju, and (d) Cape Hedo. The different color symbols with vertical lines indicated the mean and standard deviation of NO_2 TropVCD in 2015–2018, 2019, and 2020, respectively.

changes in the NO_2 TropVCD between 2015−2018 and 2020 were considerably low at −17% for Yokosuka, −25% for Busan, and −22% for Gwangju compared to those between 2019 and 2020 (−11%, −11%, and −12%, respectively), possibly because NOx emissions showed a continuously decreasing trend due to the effectiveness of regulation policies in each country (Zheng *et al.*, 2018; Kurokawa and Ohara, 2020).

Regarding monthly variations in the NO_2 TropVCD, all sites showed the typical pattern of high NO_2 in winter and low NO_2 in summer due to the longer (shorter) lifetime of NO_2 in winter (summer) associated with its photo-dissociation of NO_2 depending on the amount of solar irradiation (Kanaya *et al.*, 2014; Kroll *et al.*, 2020; Choi *et al.*, 2021). The decreased magnitudes were pronounced in May to September with high relative changes (−30% to −18%) compared to those in other months except for March and November (−3.3% to −16.4%). This finding could be partially explained by low emissions of NO_2 due to the decrease in human activity, such as activity in the transportation and industry sectors; however, the COVID-19-driven decline must be separated from these pre-existing trends, and meteorologically driven variability must be considered (Li *et al.*, 2019; Vu *et al.*, 2019; Kroll *et al.*, 2020). The difference in temperature and wind speed between 2020 and 2015 to 2019, which was measured at the nearest weather stations operated by the Japan Meteorological Agency and Korea Meteorological Agency, indicated that the warm season exhibited less favourable conditions for NO_2 photo-dissociation under relatively low temperatures (-0.41 ± 1.33°C) compared with the cool season (0.17 ± 1.59°C) along with high wind speeds (0.12 ± 0.23 m s^{-1} in the warm season vs. -0.02 ± 0.14 m s^{-1} in the cool season). In other words, lower NO_2 levels in the warm season might not have been associated with meteorological parameters, although the difference was insignificant. The detailed effects of meteorological parameters will be discussed in Section 3.3.

However, the background site, Cape Hedo, exhibited increasing trends from 2015−2018 (14%) and in 2019 (12%), suggesting that only anthropogenic emission sources decreased dramatically and that the influence of NO_2 emissions was very local due to its short lifetime under relatively high temperatures (~21°C for the annual mean temperature). Hereafter, we focus more on the three urban sites in Korea and Japan.

3.2 Time Series of the NO_2 VCD with Human Activity during the COVID-19 Period

Fig. 3 presents time series of the 15-day moving average (± 7 days) of the ground-based NO_2 TropVCD, human activity changes, and daily newly confirmed COVID-19 cases in Korea and Japan in 2020, including the periods of the Chinese New Year holiday (red shading in Fig. 3(a)) and social distancing in Korea and Japan (blue and red shading in Fig. 3(b), respectively). Google mobility data, including transit and workplace information, were used as proxies for transportation and industry, respectively. Forster *et al.* (2020) reported that the transit, workplace, retail, and residential movement data from the Google mobility trend correspond well with the surface-transportation, industry, public, and residential sector emission changes reported by Le Quéré *et al.* (2020) based on official statistics. We used the activity data of Tokyo for Yokosuka, whereas for Busan and Gwangju, we used activity data of the non-Seoul Metropolitan Area because Google did not provide the activity data for Busan and Gwangju. We assumed that the human activities in the two urban sites in Korea would correspond well with the Google mobility data of the non-Seoul Metropolitan Area because the driving activity data from Apple, which are available for Gwangju and Busan, showed moderate correlations with transit activity from the non-Seoul Metropolitan Area (0.36 for Busan and 0.45 for Gwangju).

During the Chinese New Year holiday (P2; 24−30 January 2020), the NO_2 TropVCD at the urban sites in Korea decreased rapidly by approximately −7% of the relative change in Gwangju and −31% in Busan compared to that in the previous week (P1; 16−23 January) because the NO_2 reduction during the Chinese New Year holiday period in China is a yearly phenomenon associated with decreases in business and industrial activities (Tan *et al.*, 2009; Bauwens *et al.*, 2020; Ding *et al.*, 2020; Liu *et al.*, 2020; Myllyvirta, 2020). Therefore, the NO_2 reduction in Korea, which observes the same holiday, is reasonable. However, it should be noted that the NO_2 TropVCD also decreased in Yokosuka, with a local minimum concentration after the holiday week (P3; 31 January−6 February), similar to Gwangju, although Japan does not observe the Chinese New Year holiday. The relative change of P3 to P1 in Yokosuka (−36%) was much higher than that at the

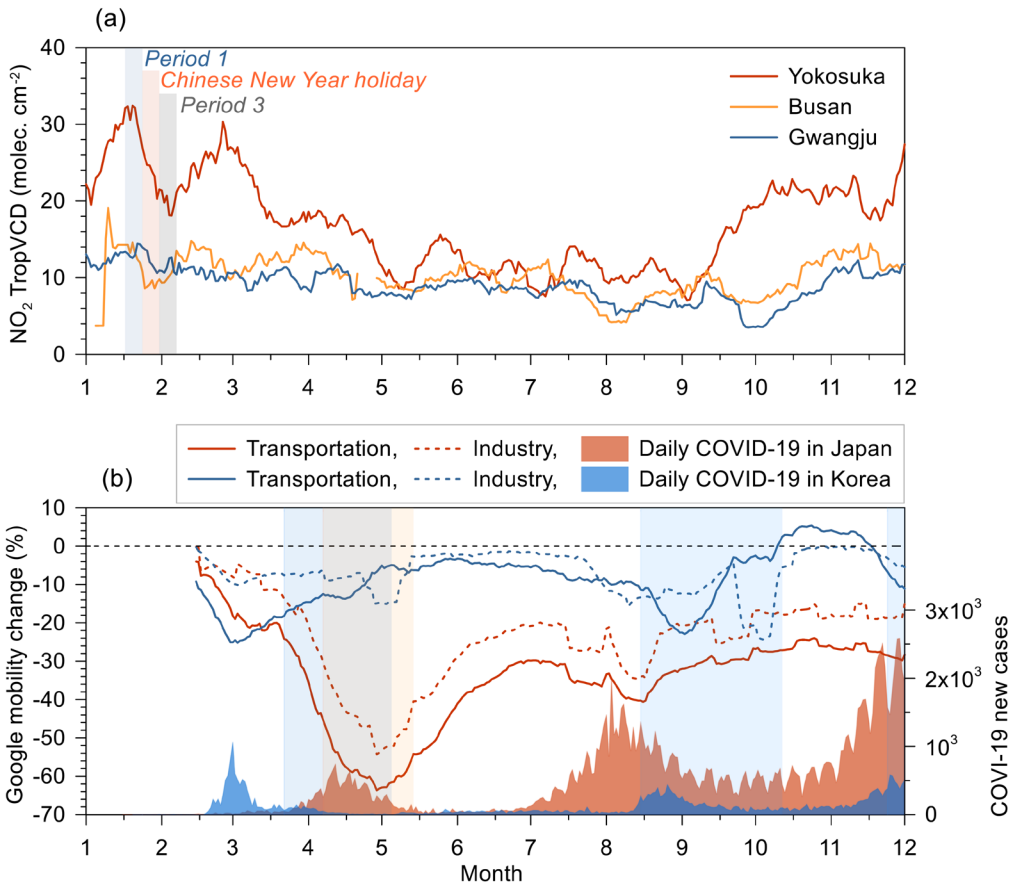

Fig. 3. (a) Time-series of 14-days running average of NO_2 TropVCD at four sites; Yokosuka, Busan, and Gwangju. The red, blue, and grey shades indicate the week of the Chinese New Year (CNY) holiday, 24–30 January in 2020, the week before (period 1) and after CNY (period 3), respectively. (b) Time-series of 14-days running average of transit and workspace from Google mobility data and daily confirmed new COVID-19 cases. The one red and three blue shade periods indicate emergency measures for social distancing in Japan and Korea, respectively.

two Korean sites (−15% at Gwangju and −25% at Busan) and even close to the change in China (−35%) (Ding *et al.*, 2020). This magnitude of the decreasing trends was similar to that for the surface NO_2 concentration recorded at an air quality monitoring station near Yokosuka (−34%).

The NO_2 reductions in this period seem to be driven solely by NO_x emissions because the difference in temperature between each period at all urban sites was not significant. Typically, a rebound in NO_2 begins approximately 7 days after Chinese New Year, the end of the holiday season (Liu *et al.*, 2020). However, the local minimum concentration in P3, not P2, revealed the ongoing reduction in human activities in both Korea and Japan. Bauwens *et al.* (2020) also reported that the strict lockdowns in Wuhan and Nanjing in China could be mainly attributed to delaying the uptick in the NO_2 concentration, unlike in previous years. After P3, the NO_2 TropVCD in Yokosuka and Gwangju recovered to levels close to those before the Chinese New Year holiday (~89%) due to the stepwise resumption of work and social activities, although the NO_2 TropVCD levels were lower than the January values, primarily due to NO_x lifetime changes as the temperature generally increased from January to February.

As new cases of COVID-19 were recognized in Korea and Japan (middle of January), the transportation and industry mobility in both countries decreased as public awareness about COVID-19 increased (Fig. 3(b)). Additionally, the NO_2 TropVCD started to decrease in accordance with the low emission rates of NO_x along with increased temperatures and decreased human activity. During the social distancing periods in Korea (March–May, August–October, and December in 2020) and Japan (April–May in 2020), Japanese mobility for transportation and industry

significantly decreased by up to –55%, whereas Korean mobility was relatively high (up to –25%). Because the measures in Korea were mostly voluntary (spontaneous social distancing while maintaining ordinary life); whereas, the Japanese government enforced emergency declaration to stay at home orders, avoid crowded places, and avoid close contacts (Azuma *et al.*, 2020; Tashiro and Shaw, 2020), resulting in conscious behavioural changes in these periods (Fig. 3(b)). In a similar context, the 15-day moving average mobility in Korea showed a much higher negative Pearson correlation coefficient (r) with newly confirmed COVID-19 cases (–0.49 for transportation and –0.36 for industry) compared to Japan (0.10 for transportation and –0.06 for industry), supporting that human activities in Korea were voluntarily restricted. Since February, based on the available Google mobility data, the 15-day moving average of the NO_2 TropVCD showed a good relationship with the transportation (r = 0.48) and industry (r = 0.54) mobility data, indicating that emissions from both major contributors to the total NO_2 burden were reduced in the Tokyo metropolitan area. In contrast, the NO_2 TropVCD at the Korean sites exhibited a moderate to low correlation with only the industrial sector (0.39 for Busan and 0.19 for Gwangju), and the transportation sector did not show a significant correlation with the NO_2 TropVCD. This is because voluntary-based social distancing in Korea might be led to a relatively small reduction of human activities which can blur their relationship. However, it is hard to exclude the other factors for the decreasing NO_2 TropVCD in Gwangju and Busan such as chemical process, long-range transport, and changes in meteorological variables (e.g., increased temperatures) that influence the lifetime of NO_2.

3.3 Deseasonalized and Deweathered Analysis

To subtract the effects of meteorological and seasonal cycles from the NO_2 TropVCD time series, the ''deweather'' package in R (Carslaw, 2018) was applied because it uses a powerful statistical technique based on boosted regression trees using the generalized boosted models (GBM) package (Ridgeway, 2020). We selected the daily averaged NO_2 TropVCD at the three urban sites from 2015 to 2020 (a total of 4466 cases), and three meteorological variables (wind speed, temperature, and relative humidity) were obtained from the nearest weather stations near the three urban sites. Then, we selected four more variables that can represent the variation in the NO_2 TropVCD: trend, week, day of week, and measurement site. The hyper parameters were tuned using a training (sample) fraction of 0.8 (3562 cases) and a validated fraction of 0.2 (891 cases). Fig. 4 shows the relationship between the predicted and measured NO_2 TropVCD values for the validation cases using the GBM model. Two variables exhibited good correlation, with an R of 0.70 and 0.85 of best-fit lines through the origin; these values were lower than those for the training cases (R = 0.81), and the mean bias and root mean squared error were low at −0.07 and

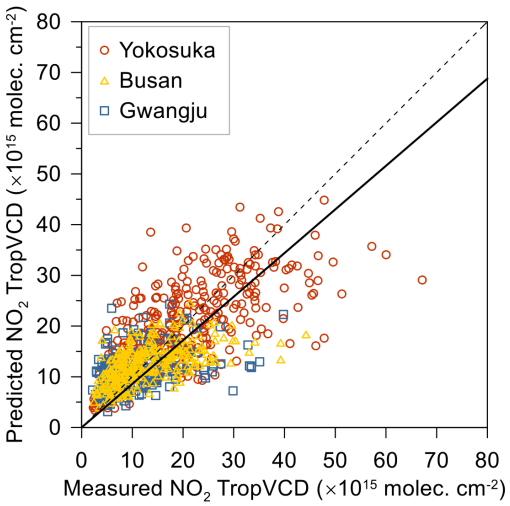

Fig. 4. Comparison of measured with predicted NO2 TropVCD which calculated from the generalized boosted (GBM) model to minimize the seasonal cycle (deseasonalized) and meteorological effects (deweathered). Different colored symbols indicate data from three urban sites (Yokosuka, Gwangju, Busan). The solid and dashed lines mean best-fit line and 1:1 line.

7.18 × 10^{15} molecules cm^{-2}, respectively, indicating that the developed model can reasonably reproduce the NO_2 TropVCD excluding meteorological effects.

Fig. 5 shows the partial dependence plots from the gradient-boosted regression models. As previously discussed, the variable with the largest influence on the NO_2 TropVCD was temperature, which is a proxy of photo-dissociation, and the next-most influential variables were the site, wind speed, trend, day of week, RH, and week of year. In the case of temperature, the NO_2 TropVCD peaked at ~5°C, not below zero, which could be suppressed condition of photo-dissociation. Considering the similar latitudes of the three urban sites, the low NO_2 TropVCD at low temperatures could be interpreted as the effect of air masses from the north passing through relatively clean areas, influenced by the Siberian continental high-pressure system during wintertime (Lee and Park, 1996; Jhun and Lee, 2004; Choi and Ghim, 2021). In contrast, the high NO_2 TropVCD at relatively high temperatures in winter might be associated with the combination of transboundary transport and stagnant conditions induced by the eastward movement of migratory high-pressure systems from China mainland (Ghim *et al.*, 2019). The highest NO_2 TropVCD was observed in Yokosuka (20.4 × 10^{15} molecules cm^{-2}), followed by those in Busan (13.1 × 10^{15} molecules cm^{-2}) and Gwangju (10.4 × 10^{15} molecules cm^{-2}), which is the same order of population and nearby strong emission

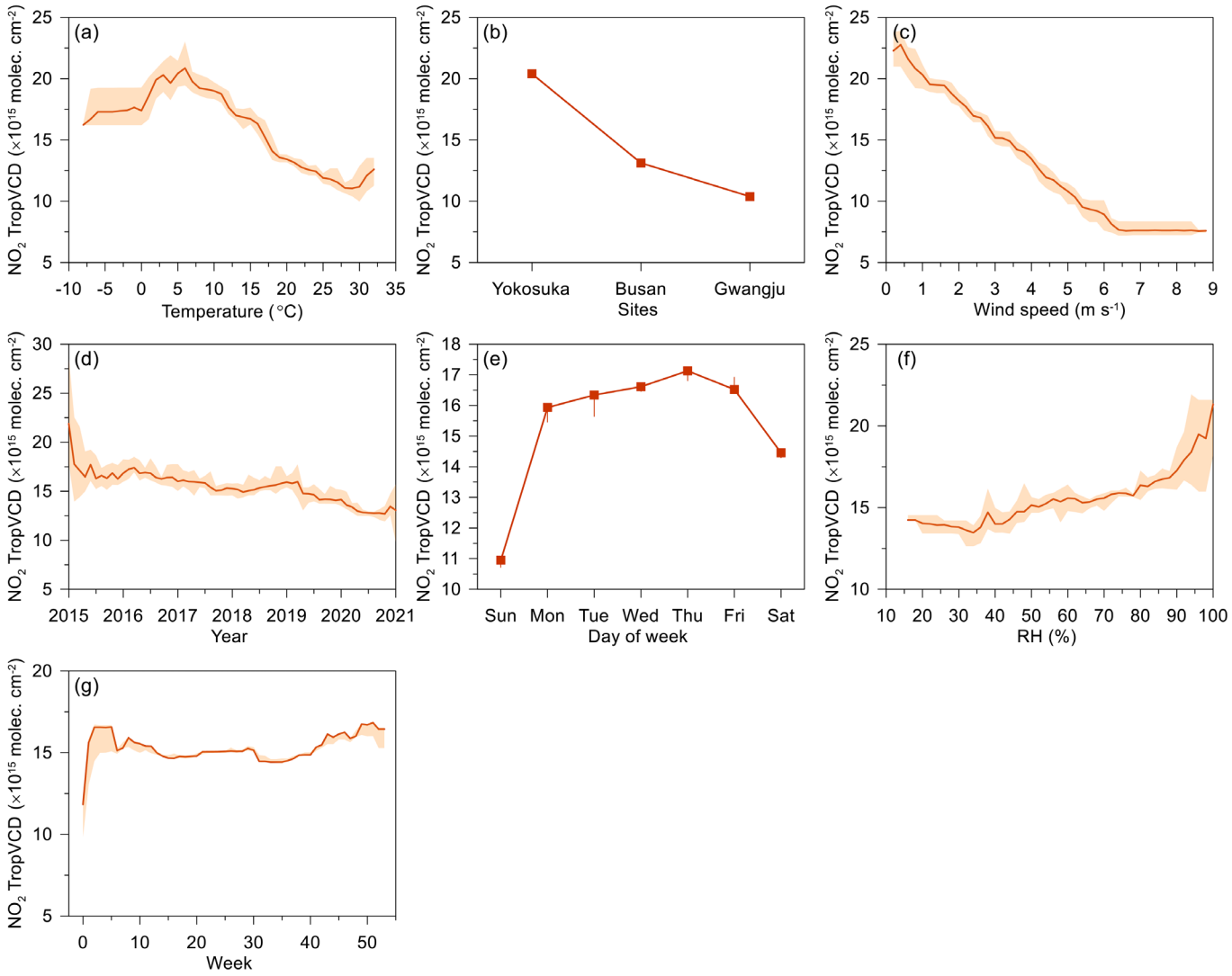

Fig. 5. The partial dependencies of each variable for predicting NO_2 TropVCD from gradient boosting from all data from three urban sites. Error shadings and vertical lines for (b) and (e) represent the standard deviation. The order of figure follows the order of influenced variables, (a) temperature (24.0%), (b) sites (20.5%), (c) wind speed (18.7%), (d) trend (11.3%), (e) day of week (10.2%), (f) RH (9.8%), and (g) week (5.4%).

sources. Wind speed was also an important variable because low wind speeds can lead to the accumulation of NO_2 emitted from human activities in urban areas. Next, the ''trend'' variable reflects a clear decreasing trend according to the air quality policies in Japan and Korea; thus, a high NO_2 TropVCD was observed in the early years of the study period (Choi *et al.*, 2021). Weekdays (Monday–Friday) exhibited a higher NO_2 TropVCD than weekends because human activities were more concentrated (Beirle *et al.*, 2003). Elevated NO_2 TropVCD levels were observed when the RH was high and during the early and late weeks of the year (winter) due to decreased photodissociation corresponding to weakened solar irradiance under cloudy (high RH) and low-temperature conditions. Therefore, the partial dependence of each variable can fully explain the NO_2 TropVCD variations at the three urban sites.

3.4 Trend Analysis with Break-point Detection

Fig. 6 shows the linear trends estimated from the Theil-Sen slope (Theil, 1950; Sen, 1968), which has been used to analyse long-term temporal variations in air quality data (Collaud Coen *et al.*, 2013; Choi and Ghim, 2021; Choi *et al.*, 2021). The Theil-Sen slope was obtained from the monthly

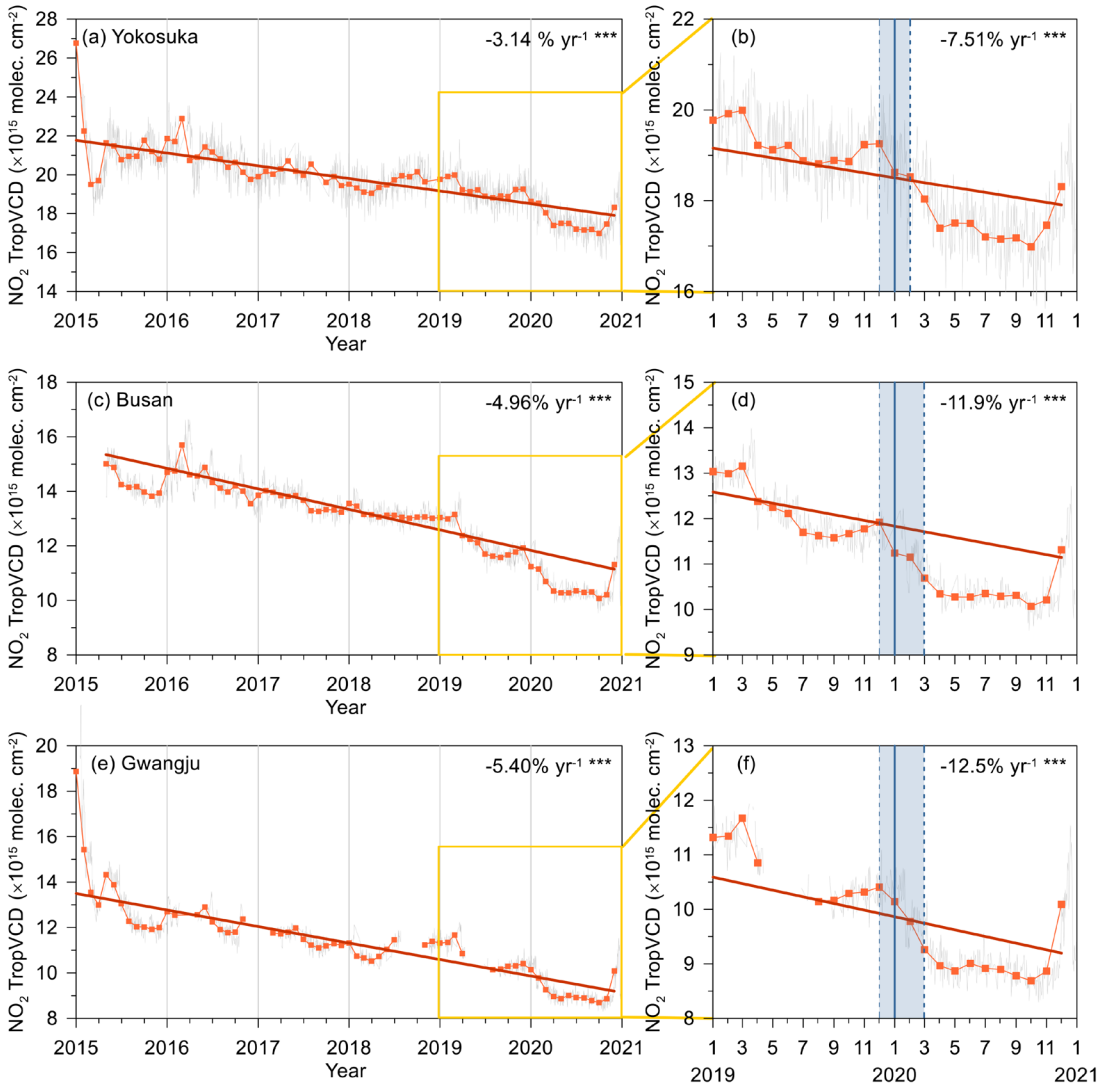

Fig. 6. The long-term trend of NO_2 TropVCD at three urban sites using deseasonalized and deweathered data using generalized boosted (GBM) model: (a) Yokosuka, (b) Busan, and (c) Gwangju. Symbols with line and solid line indicate monthly mean of NO_2 TropVCD and Theil-Sen slope from 2015 to 2020. The enlarged figures on right panel show the same as left panel except for shortening time scale (2019 to 2020). Vertical blue solid and dashed line indicate detected break-point (statistically significant changes) and 95% confidence intervals.

mean using the R function ''TheilSen'' included in the package ''openair'' (Carslaw and Ropkins, 2012). Theil-Sen analysis was used to investigate the multiyear trend of the NO_2 TropVCD based on the deseasonalized and deweathered output derived from the GBM in the previous section.

From 2015 to 2020, the Theil-Sen slope of the NO_2 TropVCD from 2015 to 2020 with a 95% confidence level continuously decreased by −5.40% yr^{-1} (−5.89 to −4.77% yr^{-1}) in Gwangju, −4.96% yr^{-1} (−5.67 to −4.3% yr^{-1}) in Busan, and −3.14% yr^{-1} (−3.56 to −2.62% yr^{-1}) in Yokosuka, and all decreasing trends were significant ($p < 0.01$). Although the considered time scales were different, the magnitudes of the decreases agreed well with results in previous studies that used ground-based instruments and/or satellites except for Gwangju (Duncan *et al.*, 2016; Herman *et al.*, 2018; Georgoulias *et al.*, 2019; Jamali *et al.*, 2020; Choi *et al.*, 2021). For the time series of the NO_2 TropVCD from 2019 to 2020, the Theil-Sen slope indicated a much steeper and significant decreasing trend (by a factor of two) than that from 2015 to 2020: −12.5% yr^{-1} (−15.4 to −9.62% yr^{-1}) in Gwangju, −11.9% yr^{-1} (−13.8 to −9.84% yr^{-1}) in Busan, and −7.51% yr^{-1} (−8.56 to −5.55% yr^{-1}) in Yokosuka ($p < 0.01$). This result is consistent with that in the previous section and reflects the dramatic decrease in the NO_2 TropVCD in 2020.

To identify the significant changes, we applied break-point analysis to the deseasonalized and deweathered NO_2 TropVCD levels using the ''strucchange'' package for break-point detection in the R program (Zeileis *et al.*, 2003), which can find a better explanation using two discrete models rather than one general model. This approach does not assume event dates but instead uses changes in linear regression properties in a data series over time to identify likely points of change by providing a more independent measure of events than a classical ''before and after'' analysis (Ropkins and Tate, 2021). Through this analysis approach, break points associated with statistically significant changes were identified in January 2020 at all three urban sites; this time frame coincides with that of the first observed cases of COVID-19 in both Korea and Japan. The 95% confidence intervals were also located in a similar range from December 2019 to February or March 2020. This result confirmed that the reduction in NO_2 was mainly due to social distancing for COVID-19 rather than annual meteorological differences. Although January 2020 overlapped with the first phase of the Korean seasonal PM control policy (December to March of the following year), the sudden reduction in NO_2, including Yokosuka, Japan, could be mainly explained by the outbreak of COVID-19. It should be noted that the decreasing trend in summer in 2020 was overwhelmed that in summer in 2019, but the NO_2 TropVCD recovered suddenly to the level in the previous year after November; this feature was also observed in the NO_2 TropVCD from OMI data.

4 CONCLUSIONS

In this study, we investigated the impact of the unprecedented COVID-19 pandemic on the NO_2 TropVCD at three urban sites (Yokosuka in Japan and Gwangju and Busan in Korea) and one remote site (Cape Hedo in Japan). Compared to the monthly mean from 2015−2018 and in 2019, that in 2020 was low due to social distancing in Korea and Japan and the lockdown in China to prevent the spread of COVID-19. At the three urban sites, the relative changes between 2015−2018 and 2020 were much larger than those between 2019 and 2020 due to the effectiveness of regulation policies, such as China's Clean Air Action. High negative relative changes were observed from May to September (−30% to −18%). The differences in temperature and wind speed between 2020 and 2015−2019 indicated that the warm season might be relatively unfavourable condition for NO_2 photo-dissociation, although an insignificant difference in the two variables blurred the effect of reduced human activity. Additionally, at Cape Hedo, no significant difference was observed between the levels in previous years and 2020, suggesting that only anthropogenic emission sources decreased dramatically.

Regarding the daily variations, the 15-day moving average of the NO_2 TropVCD during the Chinese New Year holiday at the three urban sites decreased rapidly compared to that in the previous week because the NO_2 reduction during the New Year holiday period in China is a recurring annual phenomenon associated with decreases in business and industrial activities. Japan does not observe the Chinese New Year holiday; therefore, these NO_2 reductions seemed to have been driven solely by NOx emissions at the local scale. The transportation and industry mobility levels

from the Google database in both countries decreased as public awareness about COVID-19 increased, resulting in a decrease in the NO_2 TropVCD. In the case of Yokosuka, the 15-day moving average of the NO_2 TropVCD showed notable relationships with those of transportation (0.48) and industry (0.54) mobility data. In contrast, the NO_2 TropVCD at the Korean sites showed a moderate and/or low correlation with the industrial sector (0.39 in Busan and 0.19 in Gwangju), and no significant correlation was observed for the transportation sector. These different tendencies might be associated with different social distancing policies in Korea (voluntary) and Japan (mandatory).

We applied a GBM to extract meteorological and seasonal contributions from the NO_2 TropVCD time series. The variable with the greatest influence on the NO_2 TropVCD was temperature, followed by site, wind speed, trend, day of week, RH, and week of year. Using the deseasonalized/deweathered NO_2 TropVCD from the GBM, the linear trends were estimated from the Theil-Sen slope. From 2015 to 2020, the NO_2 TropVCD at the three urban sites decreased continuously by −3.14 to −5.40% yr^{-1}. During the period from 2019 to 2020, the decreasing trend was much steeper than that from 2015 to 2020 (−7.51 to −12.5% yr^{-1}), confirming the dramatic decrease in NO_x emissions in 2020. At the three urban sites, statistically significant changes in the NO_2 TropVCD were detected in January 2020, coinciding with the first observed cases of COVID-19 in both Korea and Japan. In particular, the decreased magnitude in summer in 2020 was considerably greater than that in summer in 2019. This result confirmed that the reduction in NO_2 was mainly due to reduced NO_x emissions resulting from social distancing for COVID-19 rather than yearly meteorological differences; however, during the cold season, the NO_2 level increased notably to the previous level due to increases in human activities. In the future, model simulation should be required to understand the quantitative effects of the reduction in NO_2 emissions.

ACKNOWLEDGEMENTS

This research was supported by the GOSAT-GW NO2 NIES-JAMSTEC-NICT collaborative research project. The authors thank the City of Yokohama for maintaining the air quality monitoring stations used in this study. The MAX-DOAS data files for the MADRAS network observations from 2007 to 2021 are available at http://ebcrpa.jamstec.go.jp/maxdoashp. Pandora data at Busan were processed as part of the Pandonia Global Network (PGN; https://www.pandonia-global-network.org/, last accessed 6 November 2020). Meteorological data were obtained from the Japan Meteorological Agency and Korea Meteorological Administration through https://www.data.jma.go.jp/gmd/risk/obsdl/index.php (in Japanese) and https://data.kma.go.kr/data/grnd/selectAsosRltmList.do?pgmNo=36 (in Korean), respectively. The ground-level NO_2 concentrations in Yokohama are available at https://www.city.yokohama.lg.jp/kurashi/machizukuri-kankyo/kankyohozen/kansoku/kanshi_center/geppo/geppoarc.html (in Japanese).

REFERENCES

Azuma, K., Kagi, N., Kim, H., Hayashi, M. (2020). Impact of climate and ambient air pollution on the epidemic growth during COVID-19 outbreak in Japan. Environ. Res. 190, 110042. https://doi.org/10.1016/j.envres.2020.110042

Baldasano, J.M. (2020). COVID-19 lockdown effects on air quality by NO_2 in the cities of Barcelona and Madrid (Spain). Sci. Total Environ. 741, 140353. https://doi.org/10.1016/j.scitotenv.2020.140353

Bauwens, M., Compernolle, S., Stavrakou, T., Müller, J.F., van Gent, J., Eskes, H., Levelt, P.F., van der A, R., Veefkind, J.P., Vlietinck, J., Yu, H., Zehner, C. (2020). Impact of coronavirus outbreak on NO_2 pollution assessed using TROPOMI and OMI observations. Geophys. Res. Lett. 47, e2020GL087978. https://doi.org/10.1029/2020GL087978

Bechle, M.J., Millet, D.B., Marshall, J.D. (2013). Remote sensing of exposure to NO_2: Satellite versus ground-based measurement in a large urban area. Atmos. Environ. 69, 345–353. https://doi.org/10.1016/j.atmosenv.2012.11.046

Beirle, S., Platt, U., Wenig, M., Wagner, T. (2003). Weekly cycle of NO_2 by GOME measurements: a signature of anthropogenic sources. Atmos. Chem. Phys. 3, 2225–2232. https://doi.org/10.5194/acp-3-2225-2003

Berman, J.D., Ebisu, K. (2020). Changes in U.S. air pollution during the COVID-19 pandemic. Sci. Total Environ. 739, 139864. https://doi.org/10.1016/j.scitotenv.2020.139864

Bogumil, K., Orphal, J., Homann, T., Voigt, S., Spietz, P., Fleischmann, O.C., Vogel, A., Hartmann, M., Kromminga, H., Bovensmann, H., Frerick, J., Burrows, J.P. (2003). Measurements of molecular absorption spectra with the SCIAMACHY pre-flight model: Instrument characterization and reference data for atmospheric remote-sensing in the 230–2380 nm region. J. Photochem. Photobiol., A 157, 167–184. https://doi.org/10.1016/S1010-6030(03)00062-5

Bond, D.W., Zhang, R., Tie, X., Brasseur, G., Huffines, G., Orville, R.E., Boccippio, D.J. (2001). NO_x production by lightning over the continental United States. J. Geophys. Res. 106, 27701–27710. https://doi.org/10.1029/2000jd000191

Carslaw, D.C., Ropkins, K. (2012). *openair* — An R package for air quality data analysis. Environ. Modell. Software 27–28, 52–61. https://doi.org/10.1016/j.envsoft.2011.09.008

Carslaw, D. (2018). Deweather: Remove the Influence of Weather on Air Quality Data. https://github.com/davidcarslaw/deweather (accessed 19 August 2021)

Cede, A. (2019). Manual for Blick Software Suite 1.7. https://www.pandonia-global-network.org/wp-content/uploads/2019/11/BlickSoftwareSuite_Manual_v1-7.pdf (accessed 24 September 2022).

Chance, K.V., Spurr, R.J.D. (1997). Ring effect studies: Rayleigh scattering, including molecular parameters for rotational Raman scattering, and the Fraunhofer spectrum. Appl. Opt. 36, 5224–5230. https://doi.org/10.1364/AO.36.005224

Choi, S., Lamsal, L.N., Follette-Cook, M., Joiner, J., Krotkov, N.A., Swartz, W.H., Pickering, K.E., Loughner, C.P., Appel, W., Pfister, G., Saide, P.E., Cohen, R.C., Weinheimer, A.J., Herman, J.R. (2020). Assessment of NO_2 observations during DISCOVER-AQ and KORUS-AQ field campaigns. Atmos. Meas. Tech. 13, 2523–2546. https://doi.org/10.5194/amt-13-2523-2020

Choi, Y., Ghim, Y.S. (2021). Variations in major aerosol components from long-term measurement of columnar aerosol optical properties at a SKYNET site downwind of Seoul, Korea. Atmos. Environ. 245, 117991. https://doi.org/10.1016/j.atmosenv.2020.117991

Choi, Y., Kanaya, Y., Takashima, H., Irie, H., Park, K., Chong, J. (2021). Long-term variation in the tropospheric nitrogen dioxide vertical column density over Korea and Japan from the MAX-DOAS network, 2007–2017. Remote Sens. 13, 1937. https://doi.org/10.3390/rs13101937

Chong, H., Lee, H., Koo, J.H., Kim, J., Jeong, U., Kim, W., Kim, S.W., Herman, J.R., Abuhassan, N.K., Ahn, J.Y., Park, J.H., Kim, S.K., Moon, K.J., Choi, W.J., Park, S.S. (2018). Regional characteristics of NO_2 column densities from pandora observations during the MAPS-Seoul campaign. Aerosol Air Qual. Res. 18, 2207–2219. https://doi.org/10.4209/aaqr.2017.09.0341

Collaud Coen, M., Andrews, E., Asmi, A., Baltensperger, U., Bukowiecki, N., Day, D., Fiebig, M., Fjaeraa, A.M., Flentje, H., Hyvärinen, A., Jefferson, A., Jennings, S.G., Kouvarakis, G., Lihavainen, H., Lund Myhre, C., Malm, W.C., Mihapopoulos, N., Molenar, J.V., O'Dowd, C., Ogren, J.A., *et al.* (2013). Aerosol decadal trends – Part 1: In-situ optical measurements at GAW and IMPROVE stations. Atmos. Chem. Phys. 13, 869–894. https://doi.org/10.5194/acp-13-869-2013

Crutzen, P.J. (1970). The influence of nitrogen oxides on the atmospheric ozone content. Q. J. R. Meteorolog. Soc. 96, 320–325. https://doi.org/10.1002/qj.49709640815

Delmas, R., Serça, D., Jambert, C. (1997). Global inventory of NO_x sources. Nutr. Cycling Agroecosyst. 48, 51–60. https://doi.org/10.1023/A:1009793806086

Ding, J., van der A, R.J., Eskes, H.J., Mijling, B., Stavrakou, T., van Geffen, J.H.G.M., Veefkind, J.P. (2020). NO_x emissions reduction and rebound in China due to the COVID-19 crisis. Geophys. Res. Lett. 47, e2020GL089912. https://doi.org/10.1029/2020GL089912

Dirksen, R.J., Boersma, K.F., Eskes, H.J., Ionov, D.V., Bucsela, E.J., Levelt, P.F., Kelder, H.M. (2011). Evaluation of stratospheric NO_2 retrieved from the Ozone Monitoring Instrument: Intercomparison, diurnal cycle, and trending. J. Geophys. Res. 11, D08305. https://doi.org/10.1029/2010JD014943

Doumbia, T., Granier, C., Elguindi, N., Bouarar, I., Darras, S., Brasseur, G., Gaubert, B., Liu, Y., Shi, X., Stavrakou, T., Tilmes, S., Lacey, F., Deroubaix, A., Wang, T. (2021). Changes in global air pollutant emissions during the COVID-19 pandemic: A dataset for atmospheric modeling. Earth Syst. Sci. Data 13, 4191–4206. https://doi.org/10.5194/essd-13-4191-2021

Duncan, B.N., Lamsal, L.N., Thompson, A.M., Yoshida, Y., Lu, Z., Streets, D.G., Hurwitz, M.M., Pickering, K.E. (2016). A space-based, high-resolution view of notable changes in urban NO_x pollution around the world (2005–2014). J. Geophys. Res. 121, 976–996. https://doi.org/

10.1002/2015jd024121

Forster, P.M., Forster, H.I., Evans, M.J., Gidden, M.J., Jones, C.D., Keller, C.A., Lamboll, R.D., Quéré, C.L., Rogelj, J., Rosen, D., Schleussner, C.F., Richardson, T.B., Smith, C.J., Turnock, S.T. (2020). Current and future global climate impacts resulting from COVID-19. Nat. Clim. Change 10, 913–919. https://doi.org/10.1038/s41558-020-0883-0

Geddes, J.A., Martin, R.V., Boys, B.L., Donkelaar, A.V. (2016). Long-term trends worldwide in ambient NO_2 concentrations inferred from satellite observations. Environ. Health Perspect. 124, 281–289. https://doi.org/doi:10.1289/ehp.1409567

Georgoulias, A.K., van der A, R.J., Stammes, P., Boersma, K.F., Eskes, H.J. (2019). Trends and trend reversal detection in 2 decades of tropospheric NO_2 satellite observations. Atmos. Chem. Phys. 19, 6269–6294. https://doi.org/10.5194/acp-19-6269-2019

Ghim, Y.S., Choi, Y., Park, J., Kim, S., Bae, C.H., Seo, J., Shin, H.J., Lim, Y.J., Lyu, Y.S., Lee, Y.J. (2019). Overall characteristics of nationwide high $PM_{2.5}$ episodes during 2013~2016. J. Korean Soc. Atmos. Environ. 35, 609–624.

Herman, J., Cede, A., Spinei, E., Mount, G., Tzortziou, M., Abuhassan, N. (2009). NO_2 column amounts from ground-based Pandora and MFDOAS spectrometers using the direct-sun DOAS technique: Intercomparisons and application to OMI validation. J. Geophys. Res. 114, D13307. https://doi.org/10.1029/2009JD011848

Herman, J., Spinei, E., Fried, A., Kim, J., Kim, J., Kim, W., Cede, A., Abuhassan, N., Segal-Rozenhaimer, M. (2018). NO_2 and HCHO measurements in Korea from 2012 to 2016 from Pandora spectrometer instruments compared with OMI retrievals and with aircraft measurements during the KORUS-AQ campaign. Atmos. Meas. Tech. 11, 4583–4603. https://doi.org/10.5194/amt-11-4583-2018

Herman, J., Abuhassan, N., Kim, J., Kim, J., Dubey, M., Raponi, M., Tzortziou, M. (2019). Underestimation of column NO_2 amounts from the OMI satellite compared to diurnally varying ground-based retrievals from multiple PANDORA spectrometer instruments. Atmos. Meas. Tech. 12, 5593–5612. https://doi.org/10.5194/amt-12-5593-2019

Hermans, C., Vandaele, A.C., Fally, S., Carleer, M., Colin, R., Coquart, B., Jenouvrier, A., Merienne, M.F. (2003). Absorption Cross-section of the Collision-Induced Bands of Oxygen from the UV to the NIR, in: Camy-Peyret, C., Vigasin, A.A. (Eds.), Weakly Interacting Molecular Pairs: Unconventional Absorbers of Radiation in the Atmosphere, Springer Netherlands, Dordrecht, pp. 193–202. https://doi.org/10.1007/978-94-010-0025-3_16

Irie, H., Kanaya, Y., Akimoto, H., Iwabuchi, H., Shimizu, A., Aoki, K. (2008). First retrieval of tropospheric aerosol profiles using MAX-DOAS and comparison with lidar and sky radiometer measurements. Atmos. Chem. Phys. 8, 341–350. https://doi.org/10.5194/acp-8-341-2008

Irie, H., Takashima, H., Kanaya, Y., Boersma, K.F., Gast, L., Wittrock, F., Brunner, D., Zhou, Y., Van Roozendael, M. (2011). Eight-component retrievals from ground-based MAX-DOAS observations. Atmos. Meas. Tech. 4, 1027–1044. https://doi.org/10.5194/amt-4-1027-2011

Iwabuchi, H. (2006). Efficient Monte Carlo methods for radiative transfer modeling. J. Atmos. Sci. 63, 2324–2339. https://doi.org/10.1175/JAS3755.1

Jamali, S., Klingmyr, D., Tagesson, T. (2020). Global-scale patterns and trends in tropospheric NO_2 concentrations, 2005–2018. Remote Sens. 12, 3526. https://doi.org/10.3390/rs12213526

Jhun, J.G., Lee, E.J. (2004). A new east asian winter monsoon index and associated characteristics of the winter monsoon. J. Clim. 17, 711–726. https://doi.org/10.1175/1520-0442(2004)017<0711:Aneawm>2.0.Co;2

Judd, L.M., Al-Saadi, J.A., Janz, S.J., Kowalewski, M.G., Pierce, R.B., Szykman, J.J., Valin, L.C., Swap, R., Cede, A., Mueller, M., Tiefengraber, M., Abuhassan, N., Williams, D. (2019). Evaluating the impact of spatial resolution on tropospheric NO_2 column comparisons within urban areas using high-resolution airborne data. Atmos. Meas. Tech. 12, 6091–6111. https://doi.org/10.5194/amt-12-6091-2019

Kanaya, Y., Irie, H., Takashima, H., Iwabuchi, H., Akimoto, H., Sudo, K., Gu, M., Chong, J., Kim, Y.J., Lee, H., Li, A., Si, F., Xu, J., Xie, P.H., Liu, W.-Q., Dzhola, A., Postylyakov, O., Ivanov, V., Grechko, E., Terpugova, S., *et al.* (2014). Long-term MAX-DOAS network observations of NO_2 in Russia and Asia (MADRAS) during the period 2007–2012: Instrumentation, elucidation of climatology, and comparisons with OMI satellite observations and global model simulations. Atmos. Chem. Phys. 14, 7909–7927. https://doi.org/10.5194/acp-14-7909-2014

Koo, J.H., Kim, J., Lee, Y.G., Park, S.S., Lee, S., Chong, H., Cho, Y., Kim, J., Choi, K., Lee, T. (2020). The implication of the air quality pattern in South Korea after the COVID-19 outbreak. Sci. Rep. 10, 22462. https://doi.org/10.1038/s41598-020-80429-4

Kreher, K., Van Roozendael, M., Hendrick, F., Apituley, A., Dimitropoulou, E., Frieß, U., Richter, A., Wagner, T., Lampel, J., Abuhassan, N., Ang, L., Anguas, M., Bais, A., Benavent, N., Bösch, T., Bognar, K., Borovski, A., Bruchkouski, I., Cede, A., Chan, K.L., *et al.* (2020). Intercomparison of NO_2, O_4, O_3 and HCHO slant column measurements by MAX-DOAS and zenith-sky UV–visible spectrometers during CINDI-2. Atmos. Meas. Tech. 13, 2169–2208. https://doi.org/10.5194/amt-13-2169-2020

Kroll, J.H., Heald, C.L., Cappa, C.D., Farmer, D.K., Fry, J.L., Murphy, J.G., Steiner, A.L. (2020). The complex chemical effects of COVID-19 shutdowns on air quality. Nat. Chem. 12, 777–779. https://doi.org/10.1038/s41557-020-0535-z

Kurokawa, J., Ohara, T. (2020). Long-term historical trends in air pollutant emissions in Asia: Regional Emission inventory in ASia (REAS) version 3. Atmos. Chem. Phys. 20, 12761–12793. https://doi.org/10.5194/acp-20-12761-2020

Le Quéré, C., Jackson, R.B., Jones, M.W., Smith, A.J.P., Abernethy, S., Andrew, R.M., De-Gol, A.J., Willis, D.R., Shan, Y., Canadell, J.G., Friedlingstein, P., Creutzig, F., Peters, G.P. (2020). Temporary reduction in daily global CO_2 emissions during the COVID-19 forced confinement. Nat. Clim. Change 10, 647–653. https://doi.org/10.1038/s41558-020-0797-x

Lee, T.Y., Park, Y.Y. (1996). Formation of a mesoscale trough over the Korean peninsula during an excursion of the siberian high. J. Meteorolog. Soc. Jpn. Ser. II 74, 299–323. https://doi.org/10.2151/jmsj1965.74.3_299

Lelieveld, J., Evans, J.S., Fnais, M., Giannadaki, D., Pozzer, A. (2015). The contribution of outdoor air pollution sources to premature mortality on a global scale. Nature 525, 367–371. https://doi.org/10.1038/nature15371

Li, K., Jacob, D.J., Liao, H., Shen, L., Zhang, Q., Bates, K.H. (2019). Anthropogenic drivers of 2013–2017 trends in summer surface ozone in China. PNAS 116, 422–427. https://doi.org/10.1073/pnas.1812168116

Liu, F., Page, A., Strode, S.A., Yoshida, Y., Choi, S., Zheng, B., Lamsal, L.N., Li, C., Krotkov, N.A., Eskes, H., van der A, R., Veefkind, P., Levelt, P.F., Hauser, O.P., Joiner, J. (2020). Abrupt decline in tropospheric nitrogen dioxide over China after the outbreak of COVID-19. Sci. Adv. 6, eabc2992. https://doi.org/10.1126/sciadv.abc2992

Martin, R.V., Jacob, D.J., Chance, K., Kurosu, T.P., Palmer, P.I., Evans, M.J. (2003). Global inventory of nitrogen oxide emissions constrained by space-based observations of NO_2 columns. J. Geophys. Res. 108, 4537. https://doi.org/10.1029/2003JD003453

Miyazaki, K., Bowman, K., Sekiya, T., Jiang, Z., Chen, X., Eskes, H., Ru, M., Zhang, Y., Shindell, D. (2020). Air quality response in China linked to the 2019 novel coronavirus (covid-19) lockdown. Geophys. Res. Lett. 47, e2020GL089252. https://doi.org/10.1029/2020GL089252

Myhre, G., Shindell, D., Bréon, F., Collins, W., Fuglestvedt, J., Huang, J., Koch, D., Lamarque, J., Lee, D., Mendoza, B. (2013). Anthropogenic and natural radiative forcing. Climate change 2013: The physical science basis. Contribution of Working Group I to the Fifth Assessment Report of the Intergovernmental Panel on Climate Change, 659–740. Cambridge University Press, Cambridge.

Myllyvirta, L. (2020). Analysis: Coronavirus temporarily reduced China's CO^2 emissions by a quarter. Carbonbrief. https://www.carbonbrief.org/analysis-coronavirus-has-temporarily-reduced-chinas-co2-emissions-by-a-quarter/ (accessed 22 December 2021)

Pinardi, G., Van Roozendael, M., Hendrick, F., Theys, N., Abuhassan, N., Bais, A., Boersma, F., Cede, A., Chong, J., Donner, S., Drosoglou, T., Dzhola, A., Eskes, H., Frieß, U., Granville, J., Herman, J.R., Holla, R., Hovila, J., Irie, H., Kanaya, Y., *et al.* (2020). Validation of tropospheric NO_2 column measurements of GOME-2A and OMI using MAX-DOAS and direct sun network observations. Atmos. Meas. Tech. 13, 6141–6174. https://doi.org/10.5194/amt-13-6141-2020

Ridgeway, G. (2020). Generalized Boosted Models: A guide to the gbm package. https://cran.r-project.org/web/packages/gbm/vignettes/gbm.pdf (accessed 15 January 2022)

Rodgers, C.D. (2000). Inverse Methods for Atmospheric Sounding: Theory and Practice. World Scientific. https://doi.org/10.1142/3171

Ropkins, K., Tate, J.E. (2021). Early observations on the impact of the COVID-19 lockdown on air quality trends across the UK. Sci. Total Environ. 754, 142374. https://doi.org/10.1016/j.

scitotenv.2020.142374

Rothman, L.S., Barbe, A., Chris Benner, D., Brown, L.R., Camy-Peyret, C., Carleer, M.R., Chance, K., Clerbaux, C., Dana, V., Devi, V.M., Fayt, A., Flaud, J.M., Gamache, R.R., Goldman, A., Jacquemart, D., Jucks, K.W., Lafferty, W.J., Mandin, J.Y., Massie, S.T., Nemtchinov, V., *et al.* (2003). The HITRAN molecular spectroscopic database: edition of 2000 including updates through 2001. J. Quant. Spectrosc. Radiat. Transfer 82, 5–44. https://doi.org/10.1016/S0022-4073(03)00146-8

Sen, P.K. (1968). Estimates of the Regression Coefficient Based on Kendall's Tau. J. Am. Stat. Assoc. 63, 1379–1389. https://doi.org/10.1080/01621459.1968.10480934

Shi, X., Brasseur, G.P. (2020). The response in air quality to the reduction of Chinese economic activities during the COVID-19 outbreak. Geophys. Res. Lett. 47, e2020GL088070. https://doi.org/10.1029/2020GL088070

Takashima, H., Irie, H., Kanaya, Y., Shimizu, A., Aoki, K., Akimoto, H. (2009). Atmospheric aerosol variations at Okinawa Island in Japan observed by MAX-DOAS using a new cloud-screening method. J. Geophys. Res. 114, D18213,. https://doi.org/10.1029/2009jd011939

Takashima, H., Irie, H., Kanaya, Y., Akimoto, H. (2011). Enhanced NO_2 at Okinawa Island, Japan caused by rapid air-mass transport from China as observed by MAX-DOAS. Atmos. Environ. 45, 2593–2597. https://doi.org/10.1016/j.atmosenv.2010.10.055

Takashima, H., Irie, H., Kanaya, Y., Syamsudin, F. (2012). NO_2 observations over the western Pacific and Indian Ocean by MAX-DOAS on Kaiyo, a Japanese research vessel. Atmos. Meas. Tech. 5, 2351–2360. https://doi.org/10.5194/amt-5-2351-2012

Tan, P.H., Chou, C., Liang, J.Y., Chou, C.C.K., Shiu, C.J. (2009). Air pollution "holiday effect" resulting from the Chinese New Year. Atmos. Environ. 43, 2114–2124. https://doi.org/10.1016/j.atmosenv.2009.01.037

Tashiro, A., Shaw, R. (2020). COVID-19 pandemic response in Japan: What Is behind the initial flattening of the curve? Sustainability 12, 5250. https://doi.org/10.3390/su12135250

Theil, H. (1950). A rank-invariant method of linear and polynomial regression analysis. I, II, III,. Nederl. Akad. Wetensch., Proc. 53, 386–392, 521–525, 1397–1412, MR 0036489.

Vandaele, A.C., Hermans, C., Simon, P.C., Van Roozendael, M., Guilmot, J.M., Carleer, M., Colin, R. (1996). Fourier transform measurement of NO_2 absorption cross-section in the visible range at room temperature. J. Atmos. Chem. 25, 289–305. https://doi.org/10.1007/BF00053797

Venter, Z.S., Aunan, K., Chowdhury, S., Lelieveld, J. (2020). COVID-19 lockdowns cause global air pollution declines. PNAS 117, 18984–18990. https://doi.org/10.1073/pnas.2006853117

Vu, T.V., Shi, Z., Cheng, J., Zhang, Q., He, K., Wang, S., Harrison, R.M. (2019). Assessing the impact of clean air action on air quality trends in Beijing using a machine learning technique. Atmos. Chem. Phys. 19, 11303-11314. https://doi.org/10.5194/acp-19-11303-2019

Wagner, T., Beirle, S., Benavent, N., Bösch, T., Chan, K.L., Donner, S., Dörner, S., Fayt, C., Frieß, U., García-Nieto, D., Gielen, C., González-Bartolome, D., Gomez, L., Hendrick, F., Henzing, B., Jin, J.L., Lampel, J., Ma, J., Mies, K., Navarro, M., *et al.* (2019). Is a scaling factor required to obtain closure between measured and modelled atmospheric O_4 absorptions? An assessment of uncertainties of measurements and radiative transfer simulations for 2 selected days during the MAD-CAT campaign. Atmos. Meas. Tech. 12, 2745–2817. https://doi.org/10.5194/amt-12-2745-2019

World Health Organization (WHO) (2020). Coronavirus disease (COVID-19) outbreak. https://www.who.int/emergencies/diseases/novel-coronavirus-2019 (accessed 10 April 2020)

Zeileis, A., Kleiber, C., Krämer, W., Hornik, K. (2003). Testing and dating of structural changes in practice. Comput. Stat. Data Anal. 44, 109–123. https://doi.org/10.1016/S0167-9473(03)00030-6

Zheng, B., Tong, D., Li, M., Liu, F., Hong, C., Geng, G., Li, H., Li, X., Peng, L., Qi, J., Yan, L., Zhang, Y., Zhao, H., Zheng, Y., He, K., Zhang, Q. (2018). Trends in China's anthropogenic emissions since 2010 as the consequence of clean air actions. Atmos. Chem. Phys. 18, 14095–14111. https://doi.org/10.5194/acp-18-14095-2018